

High speed, high sensitivity MR thermometry using a balanced steady-state free precession pulse sequence

Yuan Zheng¹ and G. Wilson Miller²

¹Physics, University of Virginia, Charlottesville, VA, United States, ²Radiology and Medical Imaging, University of Virginia, Charlottesville, VA, United States

Introduction: Proton resonance frequency shift (PRFS) based thermometry techniques make use of the fact that the resonant frequency of water-based tissues varies linearly with temperature over a large temperature range [1]. Usually, temperature-sensitive images are collected using a spoiled gradient-echo (GRE) pulse sequence with relatively long echo time, allowing changes in image phase to be converted to temperature changes. However, both the sensitivity and SNR of this approach deteriorate as the imaging speed increases, which makes it less than ideal for measuring small, transient temperature changes. Thermometry using balanced steady-state free precession (bSSFP) pulse sequences has also been investigated [2,3,4]. However, in all of these approaches multiple bSSFP images need to be collected for a single temperature measurement, and the temperature sensitivity is not necessarily better than the conventional GRE method [3,4]. We have developed an alternative bSSFP-based PRFS thermometry technique that features high sensitivity, high SNR and high speed. This method is well suited for measuring small, fast, and localized temperature changes, and may therefore provide a useful complement to well-established GRE-based thermometry techniques for MR-guided focused ultrasound.

Theory: For a bSSFP pulse sequence without phase cycling, the theoretical image phase at TE=TR/2 is $\phi = \tan^{-1} \left(\frac{E_2 \sin \beta}{1 - E_2 \cos \beta} \right) + \frac{\beta}{2}$ (Eq. 1), where $E_2 = e^{-TR/T_2}$, $\beta = 2\pi\Delta f T R$, and Δf is the difference between the true resonance frequency and the operating frequency, often referred to as the off-resonance frequency. The bSSFP image phase undergoes an abrupt transition near resonance ($\Delta f = 0$ Hz) (see Fig. 1). The on-resonance phase slope is $\left. \frac{d\phi}{d(\Delta f)} \right|_{\Delta f=0} = 2\pi T_2$, resulting in higher sensitivity than the GRE method, which has a TE-dependent phase slope of $2\pi T E$. Although the bSSFP phase behavior is nonlinear in Δf and depends on the properties of the tissue (namely T_2), its functional form can easily be measured by acquiring a series of bSSFP images with different frequency offsets Δf . By performing this calibration procedure as a pre-scan, the phase changes observed during heating can be accurately converted to temperature changes over the range of frequencies spanning the bSSFP phase transition. Thus the temperature range over which this technique is applicable is limited by the bandwidth of the transition and varies with tissue type.

Methods: Experiments were performed in a hydrogel phantom using an MR-compatible 1 MHz focused ultrasound system with integrated RF coil (RK-100, FUS Instruments Inc., Toronto) and a 3T whole-body scanner (Siemens Trio). Pulse sequence parameters for all bSSFP acquisitions included: flip angle = 6° , TR/TE=4.2/2.1 ms, BW = 579 Hz/px, with in-plane resolution=1 mm and slice thickness=3 mm. We first measured the phase transition curves by acquiring a series of bSSFP images, each at a different value of Δf ranging from -50 Hz to 50 Hz. The phase transition curves at each pixel were fit to Eq. 1 and used for subsequent temperature calibration. To demonstrate that our bSSFP thermometry method can deliver quantitative accuracy similar to the conventional GRE method, we constructed a custom pulse sequence which alternated complete bSSFP image acquisitions with complete GRE acquisitions, and used this hybrid pulse sequence to monitor focal heating during a 10 W, 10 s sonication. The GRE acquisitions had the same resolution and FOV as the bSSFP scans but with flip angle= 20° , TR/TE=17.7/10 ms, BW=80 Hz/px.

To demonstrate the advantage of bSSFP over GRE for precisely measuring transient temperature rises, we used both methods to monitor focal heating due to ultrasound pulses lasting only 1 s. In one set of measurements, the frame rate of the GRE acquisition was matched to that of the bSSFP acquisition (4 images per second) by using the same TR, TE, and bandwidth. In another set of measurements, more reasonable pulse sequence parameters (TR/TE=16/7.8 ms, BW=80 Hz/pixel) were used for the GRE image acquisitions, yielding a frame rate of 1 image per second.

Results: Fig. 1 shows the measured bSSFP phase transition curve at a single pixel near the focal spot, along with a fit to Eq. 1. Fig. 2 shows the temperature evolution at the focal spot for the 10s sonication. The temperature change measured by the bSSFP method fell on the same curve as the GRE method, demonstrating the potential for a similar level of accuracy using bSSFP thermometry. Fig. 3 shows the temperature evolution at the center of the focal spot during the 1 s sonication, measured with a frame rate of 4 images per second. The bSSFP measurements clearly depict the transient focal heating at all three power levels, while the GRE measurements were dominated by noise even at the highest power. Fig. 4 shows the 2D temperature maps measured by the fast bSSFP and slow GRE pulse sequences during 1 s sonication at 10 W. The bSSFP temperature maps clearly show the rapid temperature increase and sharp, transient temperature profile across the focal spot, while the GRE temperature map fails to capture this level of detail due to its low temporal resolution.

Conclusion: We demonstrated a new PRFS thermometry technique based on a bSSFP pulse sequence, which makes use of the sharp, nonlinear phase transition of bSSFP acquisitions near resonance and features high sensitivity and high speed. This technique could be ideal for locating or characterizing the focal spot using brief, low-energy sonifications, or for precisely monitoring mild temperature rises associated with thermotherapy.

Fig. 1: bSSFP phase transition curve measured in a gel phantom.

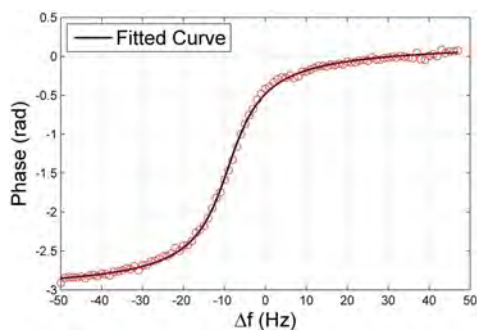


Fig. 2: Temperature evolution during 10 s, 10 W sonication measured by interleaved bSSFP/GRE image acquisitions

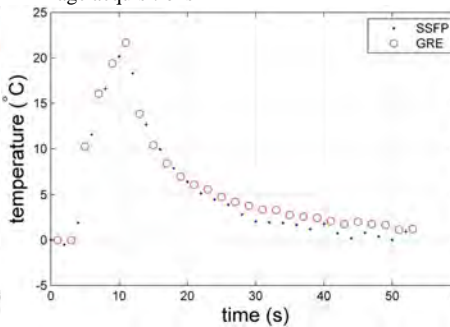


Fig. 3: Temperature evolution during 1s sonifications measured by fast bSSFP and GRE sequences.

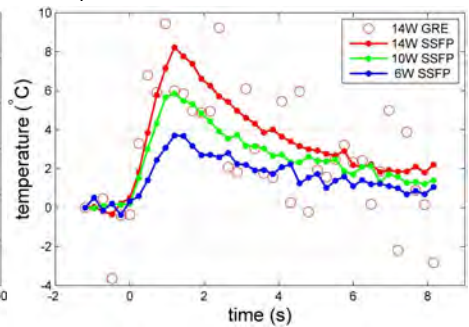
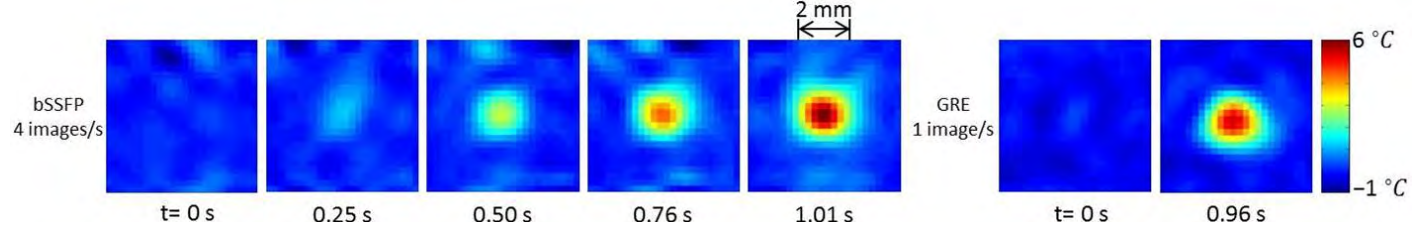


Fig. 4: 2D temperature maps during 1 s sonifications at 10 W measured by fast bSSFP and slow GRE pulse sequences.



References: [1] De Poorter J et.al. MRM 1995;33. [2] Paliwal V et. al. MRM 2004;52. [3] Scheffler K et. al. MRM 2004;51. [4] Rieke V et. al. ISMRM 2007.